COMPUTER-AIDED NOISE ANALYSIS OF INTEGRATED MICROWAVE FRONT-ENDS

Vittorio RIZZOLI (1), Diego MASOTTI (2), and Franco MASTRI (2)

(1) Dipartimento di Elettronica, Informatica e Sistemistica, University of Bologna, Villa Griffone, 40044 Pontecchio Marconi, Bologna - ITALY
(2) Istituto di Elettrotecnica, University of Bologna, Via Risorgimento 2, 40136 Bologna - ITALY

ABSTRACT

The noise performance of autonomous nonlinear subsystems including mixer/LO subassemblies is computed by a perturbative analysis of the quasi-periodic regime generated by the intermodulation of the RF signal with the autonomous local oscillation. It is shown that classical analyses based on the perturbation of the time-periodic LO regime fail to correctly describe the LO contribution to the IF noise.

INTRODUCTION

The conventional approach to noise analysis adopted in most currently available nonlinear simulators relies on the first-order perturbation of a time-periodic large-signal steady state [1], [2]. This viewpoint is not adequate for solving the basic mixer noise analysis problem, consisting in the evaluation of the near-carrier noise spectral density of the converted signal, when the mixer is fed by two noisy sinusoidal sources of known statistical properties. Only recently it has been recognized that the solution to this problem requires a perturbation analysis of the *quasi-periodic* steady state generated by the intermodulation of the two sources in the absence of noise, and an algorithm for the determination of the mixer output noise has been proposed [3].

However, for real-world microwave system simulation, the usual understanding of a mixer as a nonlinear three-port fed by two *known* sources is only an approximate model, and may represent a gross simplification of the physical reality in several practical cases. Consider for instance a receiver front-end. The RF source synthetically describes the received signal processed by a *linear* subsystem (e.g., antenna, filters, and low-noise amplifier), so that its representation by a Thévenin (or Norton) equivalent circuit is rigorously justified. However, the local oscillator is a *nonlinear* subsystem, and cannot be modeled by a simple voltage or current source. As a matter of fact, nonlinear interactions between mixer and LO may significantly modify the oscillator state equations, and thus result in considerable changes of its signal and noise performance, including the LO frequency. Thus for simulation purposes, one should always treat the mixer as integrated with the LO in a unique autonomous circuit, forced by an external sinusoidal source. The noise analysis problem then becomes considerably more difficult, and even the advanced technique discussed in [3] applies only in part.

This paper presents for the first time a general and rigorous approach to the noise analysis of mixer/LO subassemblies (or, more in general, integrated front-ends) based on the harmonic-balance (HB) principle. The quasi-periodic unperturbed (noiseless) steady state is first determined for a subassembly of arbitrary topology making use of HB algorithms for the analysis of forced oscillators [4]. The classic picture of free-running oscillator noise [2], [5] is then extended to the forced case. At relatively large frequency offsets from the carrier, noise is treated as a frequency conversion effect by a modification of the analysis method proposed in [3]. At small frequency offsets, noise is described as a consequence of direct frequency modulation of the free LO carrier operated by the noise sources, taking into account the simultaneous presence of all the mixing products generated by intermodulation (IM) with the forced RF carrier. This produces the full second-order statistics of the phase and amplitude fluctuations of all IM products of the two input frequencies, including the converted output signal. Both internal noise sources and noise injected by the RF signal are taken into account. The discussion presented in the paper is referred for clarity to the down-converter case, but the same methodology is applicable to up-converters as well, with obvious formal changes.

MODULATION NOISE AT SMALL FREQUENCY OFFSETS

Let us consider an arbitrary nonlinear circuit operating in a quasi-periodic steady state generated by the intermodulation of a free oscillation of fundamental (angular) frequency ω_{LO} and an injected sinusoidal signal of frequency ω_{RF}. ω_{LO} and ω_{RF} are considered incommensurable, and it is assumed that ω_{RF} is far enough from ω_{LO}, so that no phase locking takes place. The steady-state waveforms have spectral lines at all IM products $\Omega_{kh} = k\omega_{LO} + h\omega_{RF}$, but only a finite set of lines is retained for HB analysis purposes. Following [4], we introduce the set $\mathbf{E}$ of real and imaginary parts of the HB errors at all nonnegative Ω_{kh} and all device ports, and the state vector $\mathbf{X}$ of the real and imaginary parts of the state-variable (SV) harmonics. Since the LO regime is autonomous, the imaginary part of one harmonic at ω_{LO} is fixed to zero, and is replaced by ω_{LO} itself in the vector $\mathbf{X}$ [4]. The only free sources acting in the circuit are DC bias sources, the RF source, and noise sources whose effects are assumed to be small. Accordingly, the unperturbed steady-state vector is denoted by $\mathbf{X}_{ss}$, and the small noise-induced perturbation by $\delta\mathbf{X}$. For a spot noise analysis at a frequency offset $\omega > 0$ (from any of the steady-state harmonics), the HB circuit equations thus become

$$\mathbf{E}[\mathbf{X}_{ss} + \delta\mathbf{X}(\omega)] = \mathbf{N}_0 + \mathbf{N}_{RF} + \mathbf{N}(\omega) \tag{1}$$

where the forcing terms have been explicitly indicated for later convenience. $\mathbf{N}_0$, $\mathbf{N}_{RF}$ and $\mathbf{N}(\omega)$ are Norton equivalent representations of the DC, RF and noise sources at the n_d nonlinear-subnetwork (i.e., device) ports, respectively. From (1) we get

$$\delta\mathbf{X}(\omega) = [\mathbf{M}_{ss}]^{-1}\,\mathbf{N}(\omega) \tag{2}$$

where $\mathbf{M}_{ss}$ is the Jacobian matrix $\partial\mathbf{E}/\partial\mathbf{X}$ computed in steady-state conditions.

At small frequency offsets, PM noise is essentially generated by direct frequency modulation of the free carrier operated by the noise sources. For free-running oscillators, this classic qualitative picture [5] has been given a rigorous development in [2]. In the same work it has been shown that

TH 4B

CH3577-4/95/0000-1561$01.00 © 1995 IEEE

ordinary frequency-conversion analysis must be complemented by the modulation-noise concept in order to correctly predict the experimentally observed near-carrier PM noise. The purpose of this section is to extend this analysis to the forced oscillator case. The first step is to develop a suitable mathematical representation of the noise sources. Note that in order to compute the modulation noise, the only noise sources of interest are the internal ones, introduced by the linear subnetwork and by the nonlinear devices. The noise injected by the RF source is not considered in this analysis, for reasons to be explained later on. The internal noise sources may be globally described by a set of n_d-vectors $\mathbf{J}_{kh}(\omega)$ whose entries are complex phasors of pseudo-sinusoidal equivalent current sources at the device ports, as discussed in detail in [2]. In turn, each pseudo-sinusoid represents the noise components falling in a 1 Hz band located in the neighborhood of the sideband $\omega + k\omega_{LO} + h\omega_{RF}$ [6].

For (1) to be strictly valid in an HB environment, $\mathbf{N}(\omega)$ should represent a synchronous perturbation with spectral components at the steady-state harmonics only. Let us first consider the case of a deterministic perturbation described by an n_d-vector $\mathfrak{J}_{kh}$ of complex current phasors at each steady-state harmonic Ω_{kh}. Since in (1) the HB equations are formulated in terms of real and imaginary parts of the HB errors and of the forcing terms, in such a case the entries of $\mathbf{N}(\omega)$ would be of the form $\mathrm{Re}[\mathfrak{J}_{kh}]$, $\mathrm{Im}[\mathfrak{J}_{kh}]$, and the perturbation $\delta\mathbf{X}(\omega)$ would be deterministic, too, and time-independent. In reality, the forcing term at Ω_{kh} arises from the superposition of an upper and a lower noise sideband at $\omega \pm \Omega_{kh}$, and may thus be viewed as a sinusoidal signal at Ω_{kh} slowly modulated in both amplitude and phase at a rate ω. The time-domain waveform corresponding to the superposition of such two sidebands is given by

$$\mathrm{Re}[\{\mathbf{J}_{kh}(\omega)\exp(j\omega t) + \mathbf{J}_{-k-h}^{*}(\omega)\exp(-j\omega t)\}\exp(j\Omega_{kh}t)] \quad (3)$$

where * denotes the complex conjugate. As already mentioned, (3) is a sinusoidal signal of frequency Ω_{kh}, phase- and amplitude-modulated with a complex modulation law

$$\mathsf{J}_{kh}(t) = \mathbf{J}_{kh}(\omega)\exp(j\omega t) + \mathbf{J}_{-k-h}^{*}(\omega)\exp(-j\omega t) \quad (4)$$

Thus in the noisy case, $\mathbf{N}(\omega)$ represents a synchronous perturbation modulated at a rate ω. In order to describe the noise-modulated steady state, the constant phasors $\mathfrak{J}_{kh}$ of the above considered deterministic perturbations must be replaced by the time-dependent modulation laws (4) of the noisy perturbations. Thus in a time-domain representation of the noisy forcing terms for the autonomous system, the entries of $\mathbf{N}(\omega)$ would be of the form $\mathrm{Re}[\mathsf{J}_{kh}(t)]$, $\mathrm{Im}[\mathsf{J}_{kh}(t)]$. With this $\mathbf{N}(\omega)$, $\delta\mathbf{X}(\omega)$ would become a set of pseudo-sinusoids of frequency ω having random amplitudes and phases. In fact, equation (2) for $\delta\mathbf{X}(\omega)$ is linear, so that the linear transformations operated on $\mathbf{N}(\omega)$ automatically map onto $\delta\mathbf{X}(\omega)$ as well. Note that

$$\begin{aligned}\mathrm{Re}[\mathsf{J}_{kh}(t)] &= \mathrm{Re}[\{\mathbf{J}_{kh}(\omega) + \mathbf{J}_{-k-h}(\omega)\}\exp(j\omega t)] \\ \mathrm{Im}[\mathsf{J}_{kh}(t)] &= \mathrm{Re}[\{-j\mathbf{J}_{kh}(\omega) + j\mathbf{J}_{-k-h}(\omega)\}\exp(j\omega t)]\end{aligned} \quad (5)$$

Eqn. (5) show that we can avoid handling signals in the time domain by resorting to the customary phasor notation for representing the pseudo-sinusoidal quantities $\mathrm{Re}[\mathsf{J}_{kh}(t)]$, $\mathrm{Im}[\mathsf{J}_{kh}(t)]$. Let the entries of $\mathbf{N}(\omega)$ be replaced by the time-invariant complex phasors $\{\mathbf{J}_{kh}(\omega) + \mathbf{J}_{-k-h}(\omega)\}$, $\{-j\mathbf{J}_{kh}(\omega) + j\mathbf{J}_{-k-h}(\omega)\}$, with the rotating factor $\exp(j\omega t)$ understood. Then the entries of the perturbation vector $\delta\mathbf{X}(\omega)$ take on the meaning of complex phasors of the pseudo-sinusoidal fluctuations of the corresponding entries of the state vector $\mathbf{X}_{ss}$ in a 1 Hz band at the baseband frequency ω. In particular, the phasor of the pseudo-sinusoidal component of the LO frequency fluctuations at frequency ω is then given by

$$\delta\omega_{LO}(\omega) = \mathbf{R}\,[\mathbf{M}_{ss}]^{-1}\,\mathbf{N}(\omega) \triangleq \mathbf{T}\,\mathbf{N}(\omega) \quad (6)$$

In (6), $\mathbf{R}$ is the row matrix [0 0 0 ... 1 ... 0], whose only nonzero element corresponds to the position of the entry ω_{LO} in the state vector $\mathbf{X}$, and $\mathbf{T}$ may be interpreted as a modulation transfer matrix. The corresponding fluctuation of the generic IM product $\Omega_{kh} = k\omega_{LO} + h\omega_{RF}$ is obviously $k\,\delta\omega_{LO}(\omega)$. Since the instantaneous frequency is the derivative of the instantaneous phase with respect to time, we can express the modulation contribution to the PM noise of the generic IM product Ω_{kh} falling in a 1 Hz band at frequency ω in the following form:

$$<|\delta\Phi_{kh}(\omega)|^2> = \frac{k^2}{\omega^2}\,\mathbf{T}<\mathbf{N}(\omega)\,\mathbf{N}^{\dagger}(\omega)>\mathbf{T}^{\dagger} \quad (7)$$

where † denotes the conjugate transposed of a complex matrix. Similar perturbation techniques allow the evaluation of the AM noise and of the PM-AM correlation. As it could be expected, there is no modulation noise due to internal sources affecting the RF signal harmonics, for which k = 0. Reciprocally, the near-carrier noise of the RF source does not produce any frequency modulation of the autonomous (LO) oscillation. Thus noise injected by the RF source is always treated by the frequency-conversion technique discussed in the following section.

Note that in the presence of both thermal and flicker noise, (7) raises as ω^{-3} for $\omega \to 0$ in agreement with the measurements. On the other hand, the theory of modulation noise developed in this section is quasi-stationary, in the sense that the HB equations (1), which are strictly valid with constant forcing terms only, are formally extended to the case that the noisy forcing term has a slow sinusoidal dependence on time of the form $\exp(j\omega t)$. Thus (7) is only valid for relatively small frequency offsets (say, less than a few MHz, depending on the oscillator Q).

CONVERSION NOISE

At relatively large frequency offsets, the modulation-noise theory breaks down, and noise has to be computed by the frequency-conversion technique [3]. With this method, the signal flow among the noise sidebands $\omega + \Omega_{kh}$ is first described by a family of conversion matrices. For each steady-state harmonic, PM noise is then computed as the effect of the superposition on the carrier of a lower and an upper sideband at the same frequency offset. In this way the internally generated noise at large offsets is described as additive noise, and has a phase modulation effect, once again in agreement with the classic intuitive picture of [5]. The same applies to the noise injected by the RF source at all frequency offsets, for the reasons explained in the previous section.

A very important remark is that the frequency-conversion analysis required for the noise calculation of interest is a first-order perturbation of the *quasi-periodic* steady state generated by the intermodulation of the free oscillation with the injected RF signal. For instance, in a down converter the upper and lower LO noise sidebands $\omega \pm \omega_{LO}$ exchange power with the upper and lower IF sidebands $\omega \pm \omega_{LO} \mp \omega_{RF}$ through intermodulation with the RF signal. In a first-order perturbation analysis of the quasi-periodic steady state, this intermodulation is taken into account in the HB computation of the steady state itself, so that the power transfer from LO to IF sidebands can be correctly evaluated. On the other hand, in the conventional noise theory based on a first-order perturbative analysis of the *time-periodic* LO regime (e.g., [1]), all signals different from the LO harmonics, including the RF input, are treated as first-order perturbations. Thus intermodulation with the RF signal cannot be accounted for by this technique. As a consequence, the conventional noise analysis can only correctly evaluate the converted RF noise as far as the RF signal is small, but is unable to compute the contribution to the IF noise sidebands originating from the LO noise.

In order to carry out a frequency-conversion analysis, the original nonlinear circuit is replaced by a linearized multifrequency circuit representing its perturbative equivalent in the neighborhood of the quasi-periodic steady state. The nonlinear subnetwork is replaced by a linear multiport described by its conversion equations [3]. This multiport has a group of n_d ports associated with each sideband $\omega + k\omega_{LO} + h\omega_{RF}$. At each sideband, with the exclusion of the RF and IF ones, the n_d ports are terminated by the linear subnetwork with all external ports short-circuited. At the RF and IF sidebands, the RF and IF ports are left open, but the corresponding terminations are included in the network. The result is a linear 4-port whose admittance matrix can be evaluated by standard linear-circuit techniques.

Let us now introduce the random phasors of the pseudo-sinusoids representing the components of the noise current through the IF load, falling in 1 Hz bands located in the neighborhood of the upper and lower IF sidebands, at a frequency offset ω from the IF carrier. Such phasors will be denoted by $\delta I_{IF+}(\omega)$ and $\delta I_{IF-}(\omega)$, respectively. The IF conversion noise originates from the superposition of the converted RF noise and the internally generated noise. If the RF source is represented as a voltage generator, the RF noise can be described in terms of random complex phasors $\delta V_{\pm}(\omega)$ of pseudo-sinusoids located at the upper and lower RF noise sidebands $\omega \pm \omega_{RF}$ [6]. In the circuit linearized according to the above discussion, the output noise sidebands are linear combinations of the noise sources, so that the RF contribution may be written in the form

$$\begin{aligned} \delta I_{IF+}(\omega) &= Y_{++}(\omega)\, \delta V_{+}(\omega) + Y_{+-}(\omega)\, \delta V_{-}(\omega) \\ \delta I_{IF-}(\omega) &= Y_{-+}(\omega)\, \delta V_{+}(\omega) + Y_{--}(\omega)\, \delta V_{-}(\omega) \end{aligned} \tag{8}$$

The internally generated noise is globally described by the equivalent current noise sources $\mathbf{J}_{kh}(\omega)$ introduced in the previous section. Thus the internal contribution has the form

$$\begin{aligned} \delta I_{IF+}(\omega) &= \sum_{k,h} \mathbf{T}_{kh}^{+}(\omega)\, \mathbf{J}_{kh}(\omega) \\ \delta I_{IF-}(\omega) &= \sum_{k,h} \mathbf{T}_{kh}^{-}(\omega)\, \mathbf{J}_{kh}(\omega) \end{aligned} \tag{9}$$

In (8), (9) the $Y_{\pm\pm}(\omega)$ are conversion transadmittances, and the $\mathbf{T}_{kh}^{\pm}(\omega)$ are conversion transfer matrices. All these quantities may be evaluated by linear circuit techniques after computing the conversion matrices of the nonlinear devices by the algorithms discussed in [3]. The IF carrier PM noise at frequency ω is then related to the sideband phasors by [3]:

thermal and flicker noise, the internally generated conversion noise raises as ω^{-1} for $\omega \to 0$, which is not consistent with the measured behavior of real front-ends. For this reason, the internal noise must be described as modulation noise, and must be computed by (7), at very low frequency offsets. On the other hand, as $\omega \to \infty$ (7) tends to 0, while (10) tends to a finite limit. Thus the internal noise must be described as conversion noise, and must be computed by (9), (10) at large frequency offsets, in order to correctly evaluate the front-end noise floor. In a broad range of intermediate offsets the two results are virtually coincident, which provides a significant check of the overall physical consistency of the noise analysis technique described herein (see fig. 3).

Finally, since the IF of microwave front-ends is always relatively large (typically more than 1 MHz), frequency-conversion analysis is also used, if required, to compute the front-end noise figure [7].

APPLICATIONS

In order to illustrate the application of the noise analysis algorithms discussed in the previous sections, we consider a microwave front-end consisting of a double-balanced diode mixer combined with a simple FET oscillator, as shown in fig. 1. The RF source is an ideal voltage generator with 50 Ω internal impedance, frequency 5.48 GHz and available power P_{RF}. When loaded by an ideal 50 Ω termination, the local oscillator delivers +13.4 dBm of output power at 5 GHz, with the PM noise (computed by the method discussed in [2]) plotted in fig. 2. The PM noise of the RF source is assumed to be identical to that of the standalone local oscillator given in fig. 2.

Noise analyses are now carried out for the mixer pumped by an ideal LO source with 50 Ω internal impedance and available power +13.4 dBm, and for the actual front-end configuration shown in fig. 1. Two different RF power levels are also considered, namely, P_{RF} = -20 dBm and P_{RF} = +8 dBm, the latter approximately corresponding to the 1 dB gain compression point. The resulting PM noise of the IF carrier in each of the four operating conditions is plotted in fig. 2. In the ideal case, the near-carrier PM noise of the converted signal is simply 3 dB higher than that of each input source, due to the superposition in power of the respective uncorrelated phase fluctuations [3]. For the real front-end, a noise degradation of about 8 dB is observed, due to nonlinear mixer/LO interactions. A frequency pulling effect is also observed, with an LO frequency shift of 211 MHz at low RF levels, increasing to 223 MHz at P_{RF} = +8 dBm.

Fig. 3 shows the modulation and conversion contributions to the front-end PM noise at P_{RF} = -20 dBm. The numerical results shown in this figure agree with the indications drawn from the theoretical discussion. In particular, modulation and

$$\langle|\delta\Phi(\omega)|^2\rangle = \frac{\langle|\delta I_{IF+}(\omega)|^2\rangle + \langle|\delta I_{IF-}(\omega)|^2\rangle - 2\,\mathrm{Re}[\langle\delta I_{IF+}^{*}(\omega)\, \delta I_{IF-}(\omega)\rangle \exp(j2\phi_{IF})]}{|I_{IF}|^2} \tag{10}$$

where $I_{IF} = |I_{IF}| \exp(j\phi_{IF})$ is the phasor of the IF carrier. The AM noise and the PM-AM correlation of the IF carrier may be found in a similar way [3].

The converted RF noise is computed by replacing (8) into (10) at all frequency offsets. This calculation implies the knowledge of the statistical properties of the noisy RF source [3], which for the present purposes are considered part of the input data. The conversion contribution to the internal noise is computed by replacing (9) into (10) at large frequency offsets only. This calculation makes use of the sideband correlation matrices of the internal noise sources, which may be found in the way discussed in [2]. Note that the mean-square phase fluctuations computed by (10) are proportional to the available power of the noise sources. Thus in the presence of both

conversion noise are virtually coincident in a broad range of frequency offsets (approximately from 400 kHz up to 20 MHz). Fig. 3 also shows for comparison the results obtained from a conventional noise analysis of the front-end, based on a first-order perturbation of the time-periodic steady state generated by the local oscillation alone [1]. This technique is found to underestimate the output PM noise by more than 10 dB. A similar analysis carried out with a noiseless RF source, again reported in fig. 3, reveals that the output PM noise computed by the conventional approach is merely down-converted RF noise superimposed on the mixer noise floor.

The above results clearly show that the actual noise performance of a microwave front-end consisting of several interconnected functional blocks (primarily mixer and local oscillator), may substantially differ from the predictions generated under the assumption of ideal boundary conditions for each individual block. The analysis technique introduced in this paper may thus be indispensable in many practical cases for a realistic simulation of noise in microwave systems.

ACKNOWLEDGMENTS

This work was partly sponsored by the Italian Ministry of University and Scientific Research (MURST).

REFERENCES

[1] S. Heinen, J. Kunisch, and I. Wolff, "A unified framework for computer-aided noise analysis of linear and nonlinear microwave circuits", *IEEE Trans. Microwave Theory Tech.*, Vol. 39, Dec. 1991, pp 2170-2175.

[2] V. Rizzoli, F. Mastri, and D. Masotti, "General noise analysis of nonlinear microwave circuits by the piecewise harmonic-balance technique", *IEEE Trans. Microwave Theory Tech.*, Vol. 41, May 1994, pp. 807-819.

[3] V. Rizzoli, D. Masotti, and F. Mastri, "Full nonlinear noise analysis of microwave mixers", *1994 IEEE MTT-S Int. Microwave Symp. Digest* (San Diego), May 1994, pp. 961-964.

[4] V. Rizzoli, A. Neri, and A. Costanzo, "Steady-state analysis of forced microwave oscillators", *Proc. 21st European Microwave Conference* (Stuttgart), Sep. 1991, pp. 327-332.

[5] D. B. Leeson, "A simple model of feedback oscillator noise spectrum", *Proc. IEEE*, Vol. 54, Feb. 1966, pp. 329-330.

[6] H. E. Rowe, *Signals and noise in communications systems*. Van Nostrand: Princeton, 1965.

[7] S. A. Maas, *Microwave Mixers*. Artech House: Norwood, 1993.

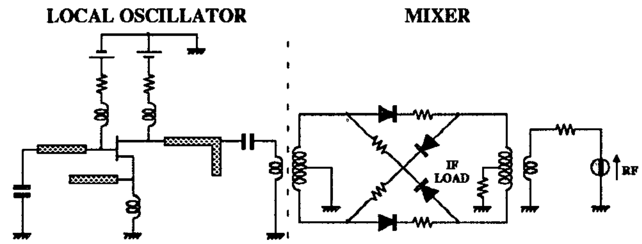

Fig.1 - Schematic topology of a real front-end

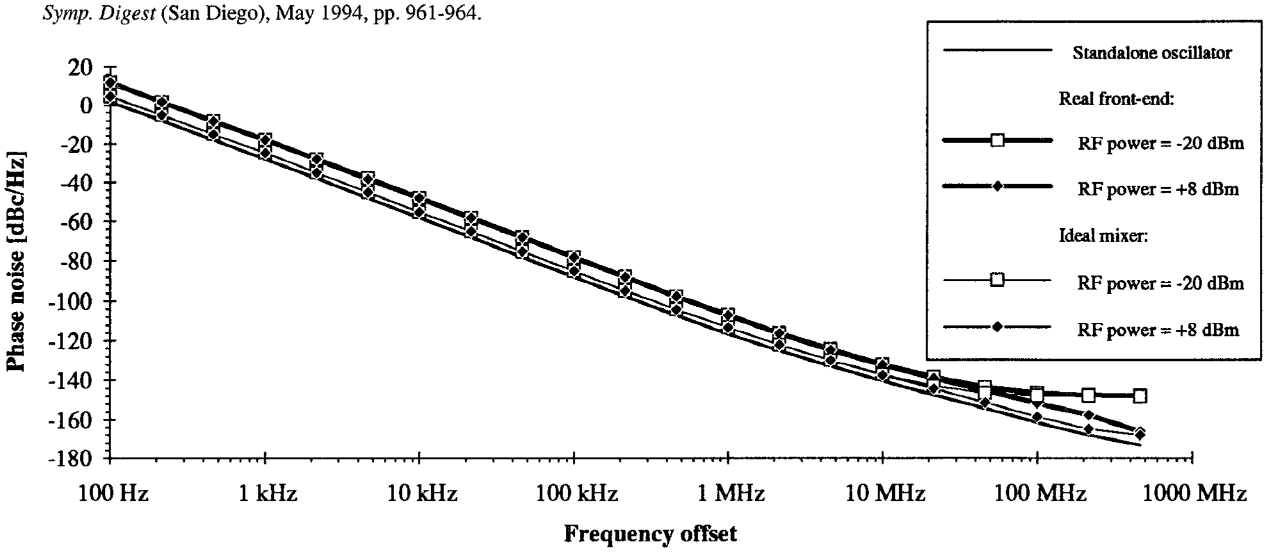

Fig. 2 - Numerical results of front-end noise analysis

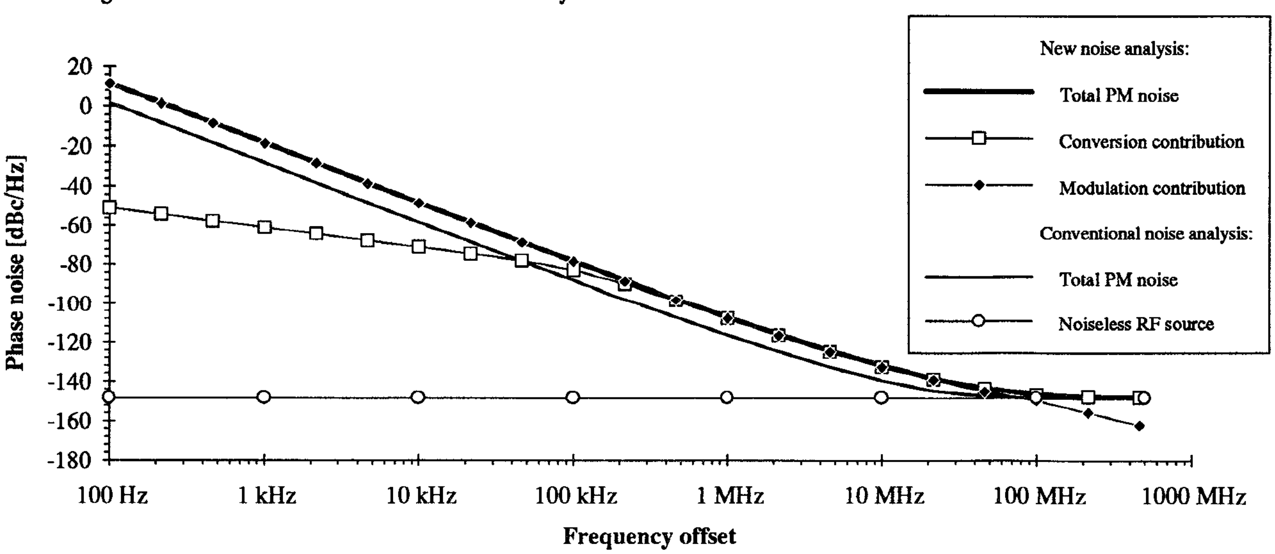

Fig. 3 - Contributions to front-end PM noise at -20 dBm of radio-frequency power